Published in final edited form as:
Environ Sci Technol. 2006 June 15; 40(12): 3941–3946.

Ultrasonically Induced Degradation of Microcystin-LR and -RR: Identification of Products, Effect of pH, Formation and Destruction of Peroxides

WEIHUA SONG[†], **ARMAH A. DE LA CRUZ**[‡], **KATHLEEN REIN**[†], and **KEVIN E. O'SHEA**[*,†]
Department of Chemistry and Biochemistry, Florida International University, University Park, Miami, Florida 33199, and Office of Research and Development, U.S. Environmental Protection Agency, Cincinnati, Ohio, 45268

Abstract

Microcystins (MCs) are a family of toxic peptides produced by a number of cyanobacteria commonly found in lakes, water reservoirs, and recreational facilities. The increased eutrophication of freshwater supplies has led to an increase in the incidence of cyanobacterial harmful algal blooms and concerns over the public health implications of these toxins in the water supply. Conventional water treatment methods are ineffective at removing low concentrations of cyanotoxins, hence specialized treatment is usually recommended for treatment of contaminated water. In this study, the products of ultrasonically induced degradation of microcystin-LR (MC-LR) and microcystin-RR (MC-RR) were analyzed by LC–MS to elucidate the probable pathways of degradation of these toxins. Results indicate preliminary products of sonolysis of MCs are due to the hydroxyl radical attack on the benzene ring and diene of the Adda peptide residue and cleavage of the Mdha–Ala peptide bond. The effect of pH on the toxin degradation was evaluated since the pH of the solution changes upon ultrasonic irradiation and varies with the water quality of treatable waters. The initial rate of MC-LR degradation is greater at acidic pH and coincides with the change in hydrophobic character of MC-LR as a function of pH. Hydrogen and organic peroxides are formed during ultrasonic irradiation, but can be eliminated by adding Fe(II). The addition of Fe(II) also accelerates the degradation of MC-LR, presumably by promoting the formation of hydroxyl radicals via conversion of ultrasonically produced H_2O_2. These findings suggest that sonolysis can effectively degrade MCs in drinking water.

Introduction

The frequency and intensity of toxic cyanobacteria blooms are increasing and present a threat to drinking water sources. The most commonly occurring toxins produced by cyanobacteria are microcystins (MCs), which are potent hepatotoxins and tumor promoters (1). MCs inhibit serine/threonine phosphatase 1 (PP1) and PP2A. This inhibition leads to the disruption of a number of critical cellular processes. In animals, the liver is the major target organ for microcystin toxicity; it was shown to accumulate 20−70% of a radioactively labeled toxin (2). MCs are normally confined within the cyanobacterial cells and are only released upon cell

*Corresponding author phone: 305−348−3968; fax: 305−348−3772; e-mail: osheak@fiu.edu..
[†]Florida International University.
[‡]U.S. Environmental Protection Agency.

Supporting Information Available
Figures showing the ultrasonic reaction apparatus; degradation of MC-LR and MC-RR (4.0 μM); effect of Fe (II) on the ultrasonic degradation of MC-LR. This material is available free of charge via the Internet at http://pubs.acs.org.

lysis (3). Animal poisoning and fish kills have been reported in conjunction with cyanobacterial blooms and have resulted in significant economic losses (1,4).

MCs are cyclic heptapeptides that share a general structure containing γ-linked D-glutamic acid, D-alanine, β-linked D-erythro-β-methylaspartic acid, *N*-methyldehydroalanine, and a unique C_{20} β-amino acid, (2S, 3S, 8S, 9S), 3-amino-9-methoxy-2,6,8-trimethyl-10-phenyldeca-4(*E*), 6(*E*)-dienoic acid (Adda), and two variable L-amino acids. The Adda moiety, present in all variants, is critical to the mode of MC activity (toxicity). Isomerization and/or oxidation of the Adda moiety dramatically reduces the toxicity associated with MCs (5). The most abundant and commonly detected microcystin in natural blooms is MC-LR (6).

The earliest case of gastroenteritis attributed to cyanobacteria was reported in 1931 in towns along the Ohio River. The water treatment processes employed over months to combat this bloom (prechlorination, sedimentation, filtration, chlorination, copper sulfate, aeration, activated carbon, permanganate, ammonia, and dechlorination), all proved to be ineffective in reducing taste, odor, or toxin content of the drinking water (7). MCs are highly stable and can withstand hours of boiling across a range of pH (8). While it is reported that MCs undergo minimal decomposition under exposure to sunlight alone, in the presence of pigments sunlight can lead to the degradation of MCs (5,9). Conventional water treatment processes have proven unreliable for the removal of these toxins and, hence, alternative treatment technologies need to be evaluated (10). Advanced oxidation processes (AOPs) have shown considerable promise for the remediation of hazardous organic compounds. AOPs involve the generation of hydroxyl radicals which effectively degrade a wide variety of pollutants. A number of studies have been reported on the application of AOPs for the degradation of MCs including TiO_2 photocatalytic degradation of MC-LR (11-13) and the activation of hydrogen peroxide by light or iron (14, 15).

Most AOPs require the addition of reagents and/or photolysis, but ultrasonic irradiation, an AOP, is reagent free and can be used for the treatment of turbid solutions and slurries. While energy costs have been the major drawback to application of ultrasound for water treatment, recent papers indicate sonochemistry may be applicable for water treatment under specific conditions or in combination with other treatments (16). A number of large-scale water and sewer treatment plants are under development and sonolytic water purification systems have entered the marketplace (17).

Ultrasonic irradiation can lead to hydroxyl radical, pyrolytic, and hydrolytic degradation processes. The degradation is highly dependent on the chemical and physical properties of the substrate. We have conducted detailed studies of different degradation pathways of MC-LR during ultrasonic irradiation and conclude that hydroxyl radical is responsible for a significant fraction of the observed degradation, but other processes, such as hydrolysis/pyrolysis, are also important (18). The hydrophobic property of MC-LR appears to play a key role during ultrasonically induced degradation. We also reported that ultrasonic irradiation effectively destroys MC-LR and its associated toxicity is dramatically decreased (18). The effect of pH on the degradation rates of MC-LR is reported herein. Significant amounts of hydrogen peroxide and organic peroxides are formed during ultrasonically induced degradation of MC-LR, but are readily degraded upon addition of Fe(II). Liquid chromatography–mass spectrometry (LC–MS) was used to identify degradation products and elucidate the pathways of toxin degradation. Preliminary products of ultrasonically induced degradation of MCs are hydroxyl radical attack on the benzene ring and diene of Adda, and cleavage of the peptide bond between Mdha and Ala. The Adda side chain, which is important for the toxicity of MCs, is readily oxidized by ultrasonic irradiation. Reaction pathways are proposed based on the LC–MS results at different irradiation times.

Experimental Section

Materials

MC-LR was purified from a laboratory culture of *Microcystis aeruginosa* CCMP 299 using the procedure previously described (18). MC-RR was purchased from Calbiochem (La Jolla, CA). The highest concentration employed for MC-RR was 0.24 mM because of its limited availability. Fe(II) sulfate heptahydrate and hydrogen peroxide 30% were obtained from Fisher Scientific, and catalase was from Sigma-Aldrich. All other reagents and solvents used were analytical or HPLC grade and all solutions were prepared in Milli-Q water. The pH of the solutions was adjusted with HCl and NaOH.

Ultrasonic Irradiation

An ultrasonic transducer UES 1.5−660 Pulsar (Ultrasonic Energy Systems, Inc.) operating at 640 kHz under operational power of 500 W equipped with a 22 mL reaction vial was fitted with a polyethylene window facing the transducer (see Figure S1, Supporting Information). The reaction vessel was centered at a distance of 4.5 cm from the face of horn. Since modest heating is observed during ultrasonic irradiation, the entire assembly was submerged in an ice bath to maintain a constant temperature of 4 °C throughout the reaction process. Samples for LC–MS analysis were prepared in 2 mL autosample vials.

Analysis

MC-LR was analyzed by HPLC with photodiode array detection under the following conditions: column, Prosphere C18 250 × 4.6 mm i.d; the mobile phase consisted of 46% CH_3OH and 54% 20 mM ammonium acetate aqueous buffer solution. The LC–MS system used in the study consisted of a Finnigan SpectraSystem P4000 HPLC Pump and Finnigan SpectraSystem As 3000 autosampler and a Thermoquest Navigator Mass Spectrometer with electrospay ionization source. The HPLC column was Alltech Prosphere C18 column (5 μm, 4.6 × 250 mm). Injection volume of the treated sample was 20 μL. Mobile phase was water and acetonitrile (ACN), both containing 0.05% trifluoroacetic acid (TFA). Gradient elution was 50% of ACN for 10 min followed by a linear increase to 85% in 5 min, held constant for addition 5 min. The mass spectra data were obtained in the positive ion mode by full scanning from *m*/*z* 600 to 1100. The hydrogen peroxide and organic hydroperoxides were determined using colorimetric methods (19).

Results and Discussion

LC–MS Identification of Byproducts from Ultrasonic Irradiation of MCs

We recently reported that ultrasonic irradiation at 640 kHz can be used to degrade MC-LR and the toxicity monitored using protein phosphatase inhibition assay (PP1) corresponds to the concentration of MC-LR (18). At an initial concentration of 4.0 μM, MC-LR and MC-RR yield similar pseudo first-order rate constants, 0.47 ± 0.06 and 0.53 ± 0.09 min^{-1}, respectively, as illustrated in Figure 2S in the Supporting Information. In an attempt to elucidate the reaction pathways and better understand the degradation process, the breakdown products were monitored using LC–MS. To separate and detect the degradation products, it is necessary to use MC concentrations much higher than those found in the environment. Rapid degradations of high concentrations of MC-LR and MC-RR were achieved upon ultrasonic irradiation (640 kHz) with 80−90% of the substrates being destroyed within 105 min as illustrated in Figure 1.

Analyses by LC–MS at various reaction times revealed ten MC-LR decomposition products at detectable levels. Our structural assignments of the breakdown products of MC-LR during ultrasonic irradiation were based on the analysis of the total ion chromatogram (TIC) and the corresponding mass spectrum. The masses of the different products were determined from the

(M + H)/z peaks corresponding to the molecular ion. For the purpose of this paper, we will refer to the products by molecular weight (MW).

For compounds with low volatility hydroxyl radical is generally considered to be the predominant oxidant during ultrasonic irradiation. Hydroxyl radical typically reacts by three competing pathways: addition, hydrogen abstraction, and electron abstraction. The rates of reaction of HO• with different reaction sites present in MC-LR are expected to vary significantly. We expect the reaction rate of hydroxyl radical addition to the aromatic ring will be fastest among the competing processes, given this process generally occurs at a nearly diffusion controlled rate (20). The H-abstraction pathways are typically slower ($\sim 10^8$ $M^{-1}s^{-1}$) and electron abstraction reaction is the least common pathway and occurs only in very electron rich systems.

Since TiO_2 photocatalytic oxidation (PCO) and sonolysis can both involve hydroxyl radical mediated degradation, we compared our LC–MS results to previously reported PCO degradation products studies (21). Different product distributions are observed from ultrasonic irradiation of MC-LR compared with the PCO studies. Products with MWs of 1029, 977, and 834 were observed during PCO and during our sonolysis studies. Liu proposed that the product with the MW of 1029 is the result of hydroxyl radical attack at the diene leading to the formation of the corresponding diol (21). The product with MW 977 is assigned to the cleavage of the cyclic peptide ring via oxidation of the Mdha moiety, while oxidative cleavage of the diene (Adda moiety) yields a product with MW 834. The assignments by Liu are consistent with the hydroxyl radical reactions expected during PCO and ultrasonic irradiation processes. Three products with MW 1011 (addition of 16 mass units) are observed within the first half-life of MC-LR during ultrasonic irradiation (Figure 2), but were not observed during PCO studies (21). The addition of 16 mass units is consistent with hydroxylation of the aromatic ring.

The reaction of hydroxyl radicals with the phenyl group in the presence of oxygen typically leads to hydroxylation yielding phenol. The addition of the electrophilic hydroxyl radical to the aromatic ring forms a resonance stabilized carbon-centered radical, subsequent addition of oxygen and elimination of a hydroperoxyl radical yields the phenolic product (22).

While the specificity of electrophilic aromatic substitution is typically governed by the nature of the substituent (20), reactions involving radicals are only modestly susceptible to substituent effects which may account for our observation of three different products with the same *m*/*z* ratio (23). The three peaks with similar retention times and MW 1011 (Figure 2) are assigned as *ortho*, *meta*, and *para* phenolic products. These products were not observed during PCO of MC-LR, presumably the result of adsorption or localization effects. Since PCO involves reactions at or near the surface, if the aromatic ring is not directly or closely associated with the surface phenolic products will not be expected. On the other hand, the phenolic products formed during ultrasonic irradiation are consistent with previously proposed localization of the phenyl group at the interface during cavitation where high concentrations of hydroxyl radicals are present (18).

We observe a product with MW 1027 which is consistent with the addition of a second hydroxyl group to the phenyl group. The addition of the hydroxyl group to the phenyl ring increases the electron rich character making it more reactive toward the addition of a second equivalent of hydroxyl radical. The product with MW 1029 corresponds to a major product and was assigned as a diol during PCO (21). This product can result from the addition of two hydroxyl radicals to the diene present in the Adda side chain. Oxidation of both the conjugated diene and phenyl ring yields a product with MW 1045 which was observed at longer irradiation time. The corresponding cleavage product (MW is 834) can be formed by oxidation of diol or cleavage

of the diene. A summary of the proposed reaction pathways involving Adda is illustrated in Figure 3.

Reaction pathways leading to opening of the MC ring have been proposed during PCO of MC-LR and we observed analogous products during ultrasonic irradiation as summarized in Figure 4. While these products can be rationalized via hydroxyl radical oxidation, pyrolysis and hydrolysis reactions can also yield these products. Pyrolysis and hydrolysis are not expected to be significant during PCO, but the extreme conditions produced by ultrasonic irradiation can lead to hydrolysis and pyrolysis of substrates localized at or near the interface during cavitation as discussed in our previous paper (18).

Product analysis of ultrasonically induced degradation of MC-RR by LC–MS revealed eight major peaks. The initial concentration of MC-RR is significantly lower than that of MC-LR, and fewer products were detected. The molecular weights of the RR products are analogous to those observed for MC-LR. The products include phenolic, diol, and ring opened adducts and we proposed hydroxyl radical pathways which are similar to those for MC-LR, summarized in Figures 3 and 4.

The reaction products of MC-LR and MC-RR were monitored using L–MS as a function of irradiation time, illustrated in Figure 5. Since the products have similar structures, we assume that their response factors (peak intensity/molecule) are similar; hence, the peak intensities are indicative of the relative yields. The early appearance of peaks assigned to the phenolic and diol products is consistent with the relative reaction rates for the hydroxyl radical reactions leading to these products compared to the other hydroxyl radical reaction pathways. The diol and phenol products of MC-LR are the major products and reach a maximum concentration after 60 min of irradiation. These initial products are readily degraded upon continued irradiation. Oxidative cleavage of the diene is also a significant reaction pathway. The oxidative cleavage of a diene can occur directly under PCO, but is also expected to be the result of hydroxyl radical reaction of the diol (secondary oxidation process). After 120 min of irradiation the major observable product of MC-LR in the reaction solution is the product from oxidative cleavage of the diene.

The reaction profile for MC-RR parallels those observed for MC-LR, with the phenol, diol, and diene cleavage products being formed in the early stages of the reaction and readily degraded upon continued irradiation. We proposed the MC-LR and -RR variants have analogous product distributions and degradation pathways under ultrasonic irradiation.

Although our studies involved only 2 of over 70 MC variants, all MCs contain the Adda moiety and should be readily degraded by ultrasonic irradiation. While mineralization may be achieved, it would require an extensive irradiation time which is not practical. It has been demonstrated that the MC byproducts from ultrasonic irradiation and PCO do not exhibit significant biological activity based on PP1 and shrimp assay protocols, hence we did not conduct mineralization studies.

Influence of pH

Since the solution pH can vary depending on the quality of water being treated, and treatment leads to acidification, the rates of degradation as a function of solution pH from 2 to 10 were studied and are summarized in Table 1. Under neutral and moderately alkaline conditions, slightly slower degradation of MC-LR was observed. The increase in the rate of degradation below pH ~4 parallels the pK_a of the carboxylic acid functionality present in MC-LR. The influence of pH on the ultrasonically induced degradation of MC-LR is similar to those observed during PCO of MC-LR (13).

Maagd et al. reported that relative hydrophobicity of MC-LR depends on pH, with the compound having the greatest log D_{ow} (octanol/water distribution ratio, analogous to K_{ow}) values under strongly acidic conditions (24). The rates of degradation as a function of pH and hydrophobicity (log D_{ow}) are summarized in Table 1. The observation that the fastest degradation occurs under the most acidic condition (greatest hydrophobicity) is consistent with the proposal that the Adda moiety (hydrophobic) is localized at the hydro-phobic interface during ultrasonically induced cavitation (18).

Role of Hydrogen Peroxide

While AOPs do not produce carcinogenic disinfection byproducts, the formation and buildup of peroxide products during AOPs is a concern. During sonolysis, relatively high local concentrations of HO• are formed and significant quantities of hydrogen peroxide can be found from hydroxyl radical combination reactions, eq 1. Sonolysis also produces organic peroxides in the presence of oxygen, as illustrated in eqs 2 and 3.

$$HO\bullet + HO\bullet \rightarrow H_2O_2 \quad (1)$$

$$RH + HO\bullet \rightarrow R\bullet + H_2O \quad (2)$$

$$R\bullet + O_2 \rightarrow ROO\bullet \rightarrow ROOH \quad (3)$$

With this in mind, we monitored the formation of peroxides during ultrasonic irradiation of MC-LR. Organic peroxides typically decompose under standard conditions used for isolation and identification, hence the total peroxide concentrations were determined by the colorimetric methods (19) as a function of irradiation time, as illustrated in Figure 6. The concentration of organic peroxides is higher than the initial concentration of MC-LR, suggesting that ultrasonic irradiation may lead to fragmentation of MC-LR via hydroxyl radical reactions and pyrolysis.

Since the H_2O_2 is a significant product of ultrasonic irradiation under our experimental conditions and H_2O_2 is often added during AOPs to improve the efficiency of the treatment process, the influence of added hydrogen peroxide was examined. Table 2 shows the degradation of MC-LR as function of added H_2O_2. These results clearly demonstrate that hydrogen peroxide at relatively high concentrations can inhibit the degradation rate of MC-LR under our experimental conditions. The reduction in observed degradation of MC-LR is likely the result of the relatively high concentration of H_2O_2 competing for the hydroxyl radical, as indicated by the following reaction scheme (20):

$$HO\bullet + H_2O_2 \rightarrow H_2O + O_2\bullet^- \quad k = 2.7 \times 10^7 \left(\mathrm{L\ mol^{-1}\ s^{-1}}\right) \quad (4)$$

Hydrogen peroxide can also undergo sonolytic degradation to yield hydroxyl radicals, but this is a relatively slow process (25). Our results indicate that the addition of H_2O_2 during ultrasonic irradiation can inhibit the degradation process. The built up ultrasonically produced H_2O_2 at longer treatment time would inhibit the degradation process.

While hydrogen peroxide has a low reactivity toward most organic pollutants, it can be converted to the strong oxidant hydroxyl radical using chemical or photochemical techniques. Fenton type chemistry involves the reduction of hydrogen peroxide by Fe(II) to produce one equivalent of hydroxyl radical (26).

$$Fe(II) + H_2O_2 \rightarrow Fe(III) + HO\bullet + HO^- \quad (5)$$

The hydrogen peroxide generated during ultrasonic irradiation can be effectively utilized when Fe(II) is added to the system, leading to an enhanced HO• generation via Fenton's reaction. Fenton oxidation has been shown to effectively decompose MCs (14,15). The initial rate of

sonolysis of the MC-LR increases modestly with Fe(II) concentration, as illustrated in Figure S3 in the Supporting Information.

In summary, the ultrasonically induced degradation of MCs appears to involve hydroxyl radical attack of the Adda benzene ring, substitution and cleavage of the Adda conjugated diene structure, and cleavage of the peptide bond between Mdha and Ala. The degradation rates increase with decreasing pH, consistent with the increase in the hydro-phobicity of MC-LR as a function of pH. Ultrasonic irradiation of MC-LR leads to significant amounts of peroxides. While the peroxides are a concern and inhibit hydroxyl radical induced degradation processes, the addition of Fe(II) can destroy the peroxides leading to hydroxyl radical, thereby improving the degradation process. The Adda moiety, which is important in MC toxicity, is readily oxidized and destroyed during ultrasonic irradiation. Although our studies involved only 2 of over 70 MC variants, all MCs contain Adda and should be readily degraded by ultrasonic irradiation. Our studies demonstrated that sonolysis can effectively and rapidly degrade MCs, but since the general application of ultrasound for water treatment is not considered to be cost-effective, careful evaluation of the economic feasibility is required prior to large scale treatment of MCs. Studies are underway to optimize the process under a variety of water quality conditions.

Acknowledgments

K.E.O. gratefully acknowledges support from the NIH/NIEHS (Grant S11ES11181). W.S. is supported by a Presidential Dissertation Fellowship from the University Graduate School at FIU. We thank the reviewers for valuable insight and suggestions.

Literature Cited

1. Hitzfeld BC, Hoger SJ, Dietrich DR. Cyanobacterial toxins: removal during drinking water treatment, and human risk assessment. Environ. Health Perspect 2000;108(suppl 1):113–22. [PubMed: 10698727]
2. Stotts RR, Twardock AR, Haschek WM, Choi BW, Rinehart KL, Beasley VR. Distribution of tritiated dihydromicrocystin in swine. Toxicon 1997;35:937–953. [PubMed: 9241787]
3. Lahti K, Rapala J, Fardig M, Niemela M, Sivonen K. Persistence of cyanobacterial hepatotoxin, microcystin-LR in particulate material and dissolved in lake water. Water Res 1997;31(5):1005–1012.
4. Andersen RJ, Luu HA, Chen D, Holmes C, Kent ML, Le Blanc M, Taylor FJ, Williams DE. Chemical and biological evidence links microcystins to salmon “netpen liver disease”. Toxicon 1993;31:1315–1323. [PubMed: 8303725]
5. Tsuji K, Naito S, Kondo F, Ishikawa N, Watanabe MF, Suzuki M, Harada K-I. Stability of microcystins from cyano-bacteria: effect of light on decomposition and isomerization. Environ. Sci. Technol 1994;28(1):173–177.
6. Vasconcelos VM, Sivonen K, Evans WR, Carmichael WW, Namikoshi M. Hepatotoxic microcystin diversity in cyanobacterial blooms collected in portuguese freshwaters. Water Res 1996;30(10):2377–2384.
7. Tisdale ES. Epidemic of intestinal disorders in Charleston, W. VA., occurring simultaneously with uprecedented water supply conditions. Am. J. Public Health 1931;21:198–200.
8. Harada KI, Tsuji K, Watanabe MF, Kondo F. Stability of microcystins from cyanobacteria-III, effect of pH and temperature. Phycologia 1996;35(6):83–88.
9. Tsuji K, Watanuki T, Kondo F, Watanabe MF, Suzuki S, Nakazawa H, Suzuki M, Uchida H, Harada K-I. Stability of microcystins from cyanobacteria-II. Effect of UV light on decomposition and isomerization. Toxicon 1995;33(12):1619–1631. [PubMed: 8866619]
10. Keijola AM, Himberg K, Esala AL, Sivonen K, Hiisvirta L. Removal of cyanobacterial toxins in water treatment processes: laboratory and pilot-scale experiments. Toxicol. Assess 1988;3(5):643–656.

11. Lawton LA, Robertson PKJ. Physicochemical treatment methods for the removal of microcystins (cyanobacterial hepatotoxins) from potable waters. Chem. Soc. Rev 1999;28:217–224.
12. Lawton LA, Robertson PKJ, Cornish BJ, Jaspars M. Detoxification of microcystins (cyanobacterial hepatotoxins) using TiO_2 photocatalytic oxidation. Environ. Sci. Technol 1999;33(5):771–775.
13. Feitz AJ, Waite D, Jones GJ. Photocatalytic degradation of the blue green algal toxin microcystin-LR in a natural organic–aqueous matrix. Environ. Sci. Technol 1999;33(2):243–249.
14. Bandala ER, Martinez D, Martinez E, Dionysiou DD. Degradation of microcystin-LR toxin by Fenton and photo-Fenton processes. Toxicon 2004;43(7):829–832. [PubMed: 15284017]
15. Gajdek P, Lechowski Z, Bochnia T, Kepczynski M. Decomposition of microcystin-LR by Fenton oxidation. Toxicon 2001;39:1575–1578. [PubMed: 11478965]
16. Mason TJ, Joyce E, Phull SS, Lorimer JP. Potential uses of ultrasound in the biological decontamination of water. Ultrason. Sonochem 2003;10(6):319–323. [PubMed: 12927606]
17. Mason, TJ.; Tiehm, A. Ultrasound in Environmental Protection, Advances in Sonochemistry. Jai; Amsterdam: 2001.
18. Song W, Teshiba T, Rein K, O'Shea KE. Ultrasonically induced degradation and detoxification of microcystin-LR (Cyanobacterial toxin). Environ. Sci. Technol 2005;39:6300–6305. [PubMed: 16173596]
19. Gere EP, Berczi B, Simandi P, Wittmann G, Dombi A. Simultaneous determination of hydrogen peroxide and organic hydroperoxides in water. Inter. J. Environ. Anal. Chem 2002;82(7):443–450.
20. Buxton GV, Greenstock CL, Helman WP, Ross AB. Critical review of rate constants for reactions of hydrated electrons, hydrogen atoms and hydroxyl radicals ($\cdot OH/\cdot O^-$) in aqueous solution. J. Phys. Chem. Ref. Data 1988;17(2):513–886.
21. Liu I, Lawton LA, Robertson PKJ. Mechanistic studies of the photocatalytic oxidation of microcystin-LR: an investigation of byproducts of the decomposition process. Environ. Sci. Technol 2003;37(14): 3214–3219. [PubMed: 12901672]
22. Kurata T, Watanabe Y, Katoh M, Sawaki Y. Mechanism of aromatic hydroxylation in the Fenton and related reactions. One-electron oxidation and the NIH shift. J. Am. Chem. Soc 1988;110(22):7472–7478.
23. O'Shea KE, Cardona C. Hammett study on the TiO_2-catalyzed photooxidaiton of para-substitued phenol. A kinetic and mechanistic analysis. J. Org. Chem 1994;57(17):5005–5009.
24. Maagd PD, Jan Hendriks A, Seinen W, Sijm THM. pH-Dependent hydrophobicity of the cyanobacteria toxin microcystin-LR. Water Res 1999;33(3):677–680.
25. Gogate PR, Pandit AB. A review of imperative technologies for wastewater treatment II: hybrid methods. Adv. Environ. Res 2004;8(3−4):553–597.
26. Walling C. Fenton's reagent revisited. Acc. Chem. Res 1975;8(4):125–131.

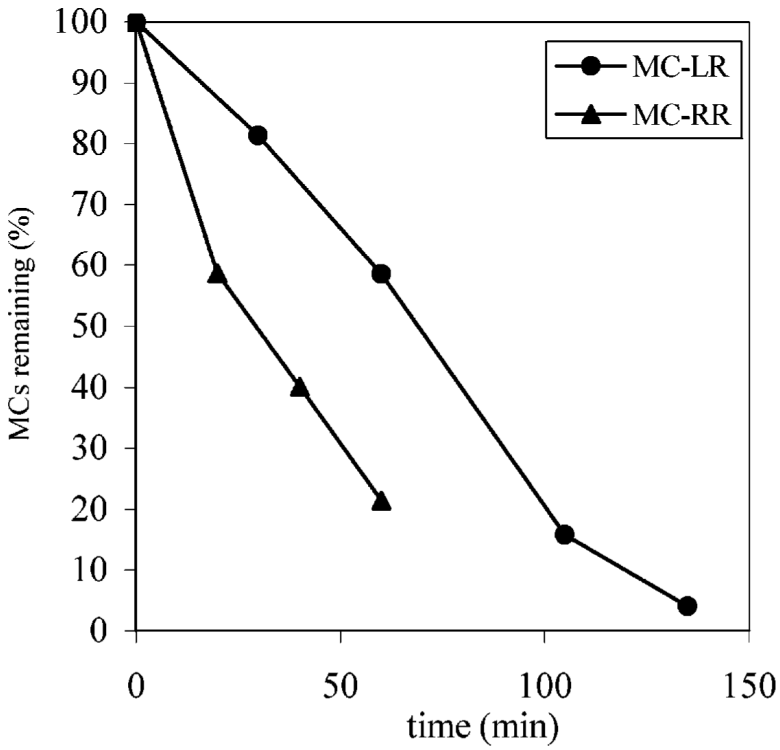

FIGURE 1.

Destruction of MC-LR and MC-RR by ultrasonic irradiation monitored by LC-MS. The initial concentrations of MC-LR and MC-RR are 1.0 and 0.24 mM, respectively. The reproducibility of the analytical measurements is within 5% on the basis of triplicate runs.

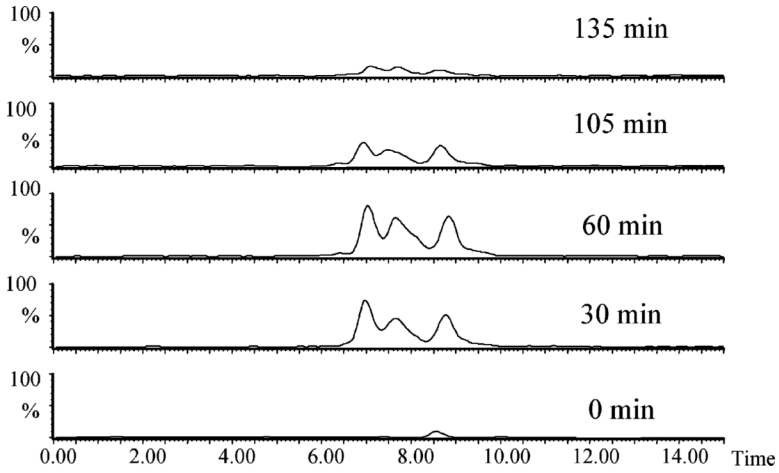

FIGURE 2.

LC-MS analysis data for the decomposition products of MC-LR under ultrasonic irradiation. Selective ion mass chromatograms monitored at *m/z* 1012 at different reaction time.

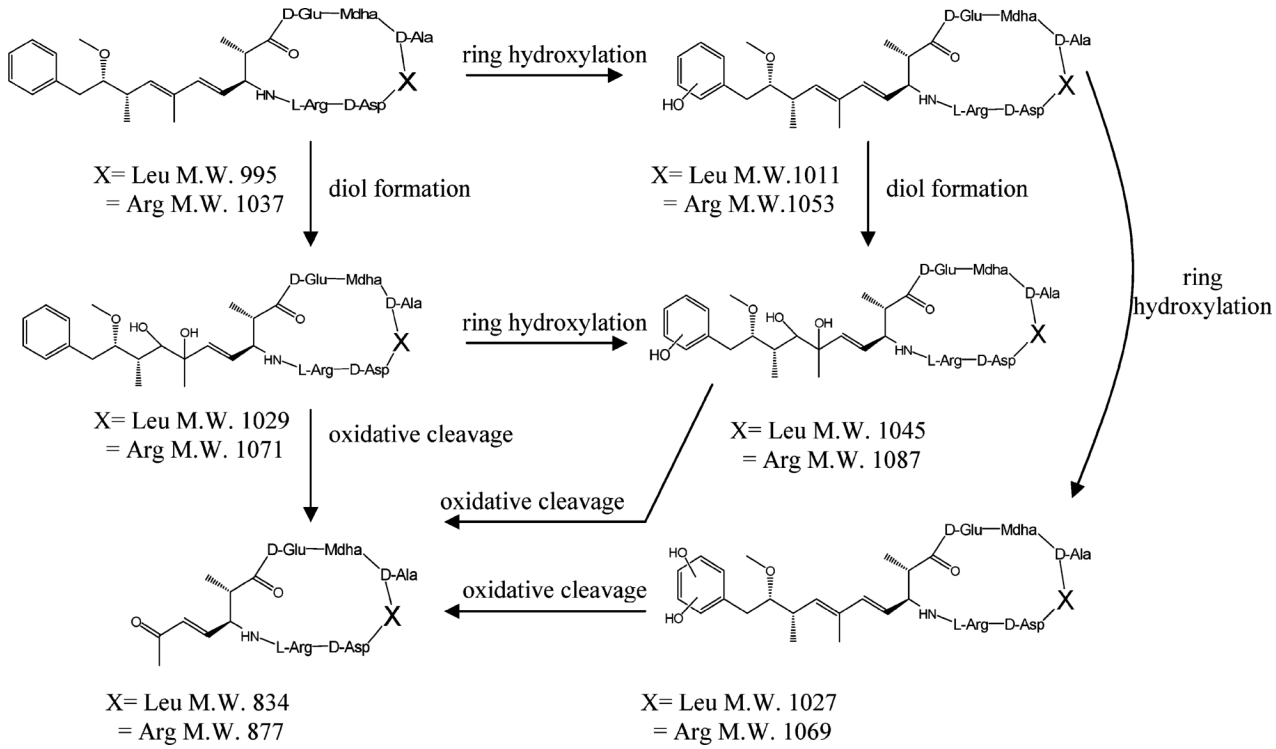

FIGURE 3.

Byproducts and proposed reaction pathways for ultrasonically induced degradation of the Adda side chain of MC-LR (X = Leu), MC-RR (X = Arg).

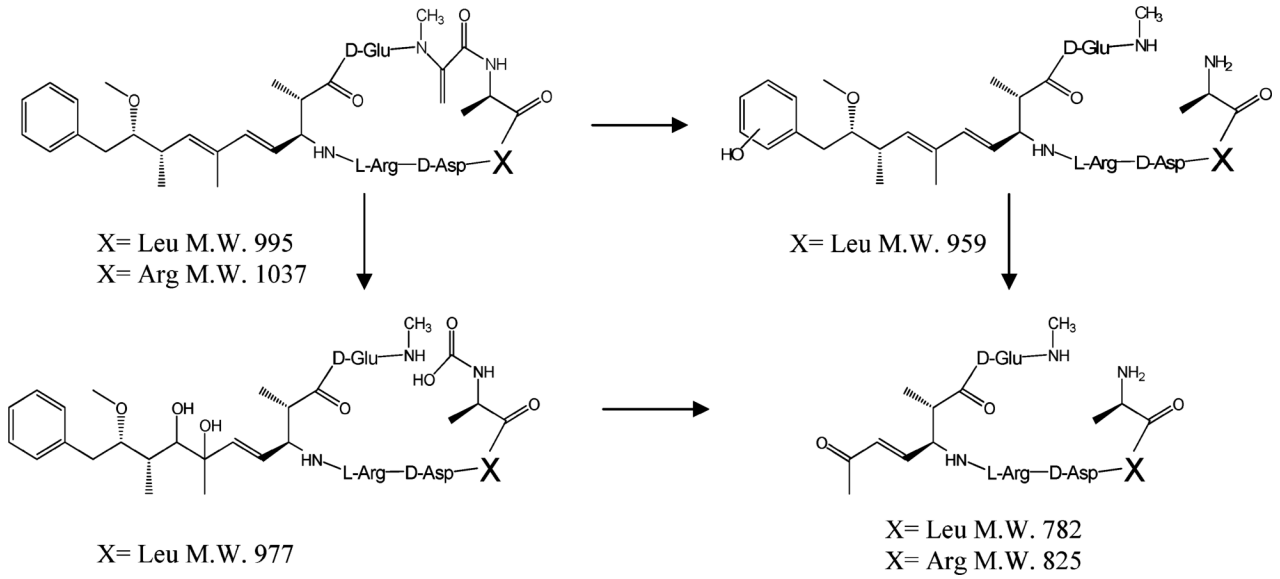

FIGURE 4.

Byproducts and proposed reaction pathways for ultrasonically induced degradation of the cyclic region of MC-LR (X = Leu), MC-RR (X = Arg).

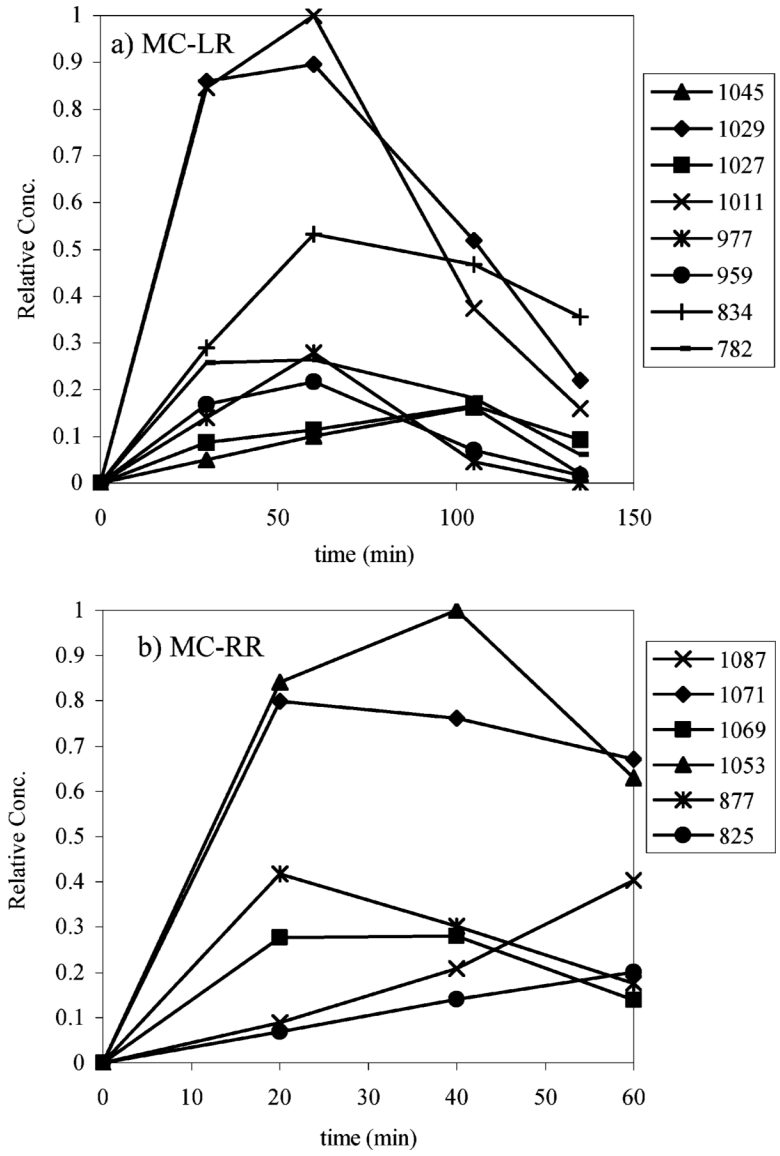

FIGURE 5.
Reaction profile of byproducts (listed by MW) from ultrasonically induced degradation of MC-LR and MC-RR.

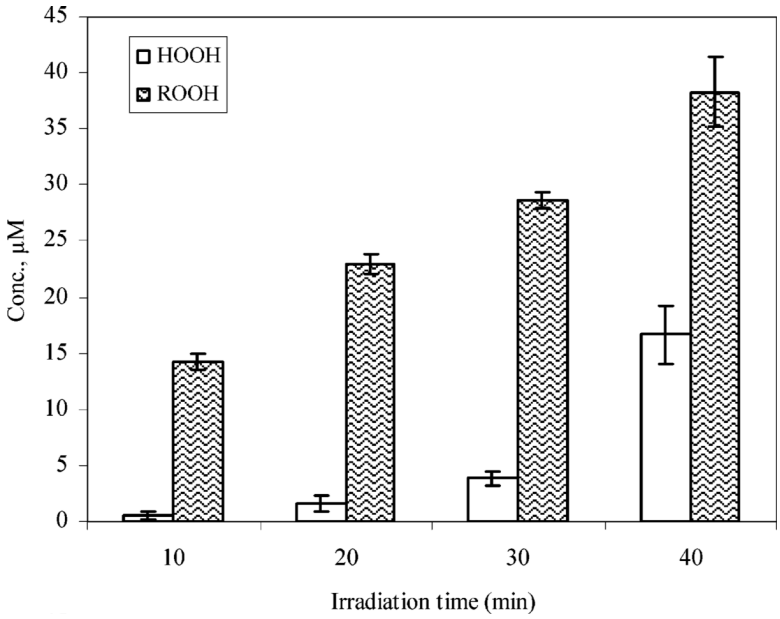

FIGURE 6.

Formation of peroxides from ultrasonically induced degradation of MC-LR. The initial concentration of MC-LR is 10 μM. Analyses were preformed in triplicate and the error bars indicate the standard deviation of the mean.

TABLE 1

Ultrasonically Induced Degradation Rates of MC-LR at Various Solution pHs, Parallel the Hydrophobicity of MC-LR (Initial MC-LR Concentration was 3.0 μM)

pH of the solution	degradation rate of MC-LR (min^{-1})[a]	Log D_{ow}[b]
2.3	>3.0	1.5
3.2	1.01 ± 0.09	1.2
3.8	0.47 ± 0.02	1.0
4.7	0.66 ± 0.20	0
5.6	0.44 ± 0.15	−0.2
9.7	0.48 ± 0.04	−1.8

[a] Observed first-order exponential decay rate (min^{-1}). The reproducibility of the individual data points is within 5% based on triplicate runs. The reported uncertainty is based on the standard deviation.

[b] Values were extrapolated from ref 24.

TABLE 2

Effect of H_2O_2 on the Ultrasonically Induced Degradation of MC-LR (Initial Concentration of MC-LR was 4.0 μM)

concentration of H_2O_2 (mM)	degradation rate of MC-LR (min^{-1})[a]	R^2
0	0.47 ± 0.06	0.995
3.0	0.29 ± 0.01	0.999
15	0.15 ± 0.07	0.985
30	0.13 ± 0.03	0.997

[a] Observed first-order exponential decay rate (min^{-1}). The reproducibility of the individual data points is within 5% based on triplicate runs. The reported uncertainty is based on the standard deviation.